Preliminary Study of Breast Cancer Detection Using A Computational Microwave Imaging System

Rupesh Kumar[#1], Vincent Fusco[#2], Okan Yurduseven[#3]
[#]Centre for Wireless Innovation, Queen's University Belfast, UK
{[1]Rupesh.Kumar, [3]Okan.Yurduseven}@qub.ac.uk, [2]v.fusco@ecit.qub.ac.uk

***Abstract*— In this paper, a preliminary study related to the detection of breast cancer based on a computational microwave imaging system is presented at K-band frequencies. In comparison to normal tissues, the different dielectric properties (permittivity and conductivity) of the malignant tissues can be exploited in order to detect the presence of tumour through a microwave imaging system. This work demonstrates the detection of breast tumour as an application of a computational imaging technique by leveraging the concept of the dynamic metasurface antenna (DMA) aperture as a transmitter. In this framework, the computational imaging aperture can provide a compact system design with a low-cost deployment for detecting tumours in early-stage, and this can speed up the screening process of the population at risk. Particularly, early detection of Stage 1 can help with the determination of the best treatment method and enhance a patient's prognosis.**

***Keywords*— Breast cancer, computational imaging, dynamic metasurface antenna, simulation, sensing matrix.**

I. Introduction

Microwave imaging has a tremendous potential in the deployment of medical imagining systems capable of detecting malignant tissues within the breast. Currently, the widely used diagnostic systems such as magnetic resonance imaging (MRI), X-ray. In case of X-ray mammography, it poses many health risks due to its ionising radiation. For MRI, a high operating cost is also considered as one of the main drawbacks. Additionally, the long examination times and limited access to these imaging systems make it unsuitable for early-stage breast cancer detection for the screening of the population at risk. According to Cancer Research UK [1], [2], around 55,900 new breast cancer cases were registered in the UK between 2016-2018, that is more than 150 cases being reported every day. The incidence rates for breast cancer are projected to be 210 cases per 100,000 females by 2035. On these issues, microwave imaging technology has potential to address the limitations of today's standard imaging modalities for breast cancer detection.

This work presents the preliminary study of a computational microwave imaging technique which can be utilized for detecting the malignant tissues in breast tumour at K-band frequencies. The presented system has used the concept of a dynamic metasurface antenna (DMA) and eight open-ended waveguide probes (WR42) as a transmit and receive units, respectively. This study is interested in providing a computational solution to image the tumour in early-stage of their growth. The focus of this work is to use the difference in the dielectric properties of a risky breast tissues. Normally, the dielectric properties of the malignant tissues in breast cancer have different values compared to the normal tissues [3], [4]. This difference helps in detection by the imaging technique [5]. Additionally, microwave imaging employs unharmful low-level energy levels and has lower costs than the widely used medical tools. In the case of ultrasound, the images are less effective in distinguishing the malignant from the normal tissues. Therefore, the microwave imaging system has potential to replace the existing detection modalities with a low-cost solution.

Leveraging an active microwave imaging scenario, the breast-under-investigation is illuminated by the microwave signals. Then, the reflected signals are post-processed to reconstruct an image of the breast structure. In this paper, the dynamic nature of DMA is utilized here to synthesize the required quasi-random radiation patterns to facilitate computational imaging. The DMA makes use of a single-channel, constituting a single-pixel hardware architecture on the transmitter side. The study of DMA is performed in a full-wave Microwave Studio CST over 20 GHz – 22 GHz band frequencies. This frequency band is considered to see the performance of the microwave as a preliminary study.

The rest of the paper is organized as follows. In Section II, we present the computational imaging model and formulate the imaging problem. Section III discusses the DMA aperture as well as the modelling of the breast-tumour for computational imaging. Finally, Section IV presents the simulated results while the concluding remarks are presented in Section V.

II. Computational Imaging

A. Theory of Computational Imaging

The computational imaging process is presented in detail in [6] and is depicted in Fig. 1. The near-field scan aperture is located at 5λ (21 GHz) from the transmit and receive antenna aperture plane, and the scene is at 7λ from the near-field plane.

The computational imaging involves two main steps which are simulated in the full-wave Microwave Studio CST. First is the spatial scanning of near electric-fields and second is the backscattered signals due to all radiating modes probing the scene information. For near electric-field scanning, the first-Born approximation is considered for constructing the sensing matrix. Therefore, the sensing matrix is constructed by a linear combination of the electric fields, ETx and ERx.

Here, ETx and ERx denote the electric fields radiated by the considered transmit-and-receive pairs. After the electric-field scanning, the second step is implemented by performing the simulation of all backscattered signals corresponding to each of the steps/measurements. From now onwards, we have used the word 'measurement' synonymously for the 'step' involved in the computational imaging.

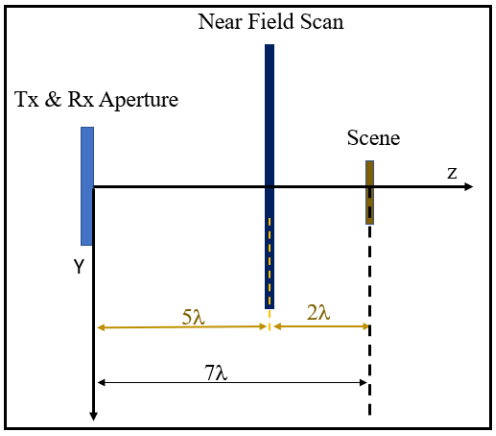

Fig. 1. Configuration of the computational imaging system.

The above computational steps are mathematically associated to the scene reflectivity, f, and it can be represented as,

$$\mathbf{g}_{M\times 1} = \mathbf{H}_{M\times N}\mathbf{f}_{N\times 1} + \mathbf{n}_{M\times 1} \tag{1}$$

where, g is the simulated backscattered signals, H is the sensing matrix, and n is the noise. Here, the scene reflectivity, f, can be estimated by means of any known computational reconstruction algorithms, such as matched-filter and least-squares. In (1), M denotes the number of considered measurements associated to all Tx-Rx pairs to sample the scene information whereas N is the number of pixels used to represent the scene. In this work, the matched-filter technique is used for image reconstructions. Using matched filtering, the imaged scene can be reconstructed as:

$$\mathbf{f_{est}} = \mathbf{H}^{\dagger}\mathbf{g} \tag{2}$$

where the symbol † denotes the Hermitian transpose operator. In medical imaging, the reconstructed image of a scene is governed by the reflectivity of tissues, hence the computational imaging can also be used to reconstruct the malignant tissues. This way, the reconstructed image detects the malignant tissues within the breast structure.

B. Transmit and Receive Aperture Plane

The transceiver aperture plane is illustrated in Fig. 2. It consists of a single DMA (Tx in blue colour) aperture and eight receive (Rx in red colour) antennas. The length between two successive probes is 2.5λ which is selected to cover each side of the DMA by three probes in order to keep the setup simple, see Fig. 6. This forms a square plane with the DMA at its centre.

1) Transmitter: DMA Aperture

The DMA architecture is presented in Fig. 3

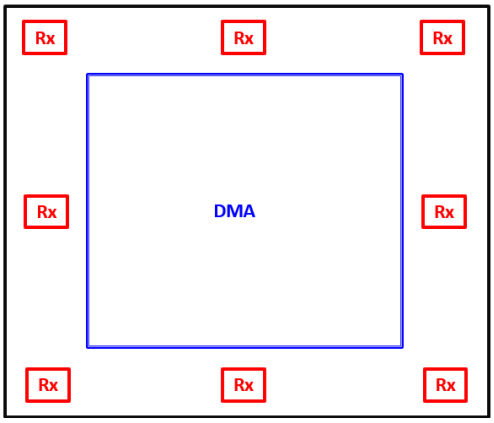

Fig. 2. Configuration of the DMA and the receiver probes as a transceiver.

The electrical size of the DMA is 4λ. The DMA consists of a parallel-plate waveguide with the copper cladding on the top and bottom layers of substrate. The substrate material is Rogers R04003C ($\epsilon_r = 3.55$, $tan\delta = 0.0027$, $thickness = 0.152mm$). All edges are fenced with the copper layer. The top layer has an array of sub-wavelength sampled circular complementary electric-LC (CcELC) metamaterial elements. The metamaterial elements are designed to operate between 20-22 GHz band. Each CcELC element has a narrow resonance band frequency within the operating frequency band like in [7]. Excitation of the metasurface layer is achieved through a coaxial probe located at the centre as marked in Fig. 3.

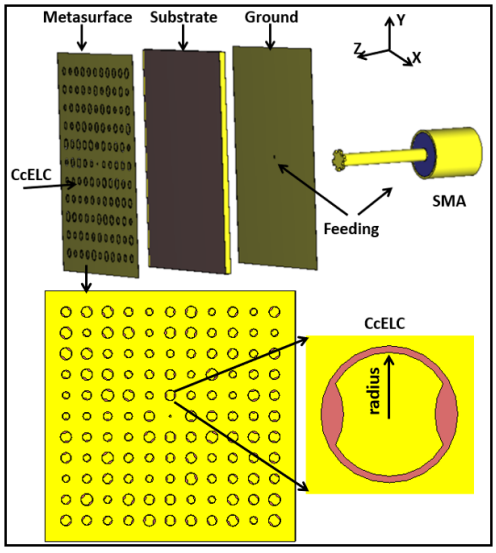

Fig. 3. Example of a mask from DMA's configuration.

As the operating frequency is swept between 20-22 GHz, at each frequency, only a certain subset of CcELC metamaterial

elements couple to the guided-mode launched inside the dielectric substrate. Because the resonance frequencies of the CcELC elements across the DMA aperture are distributed on a random basis, at each frequency, the DMA radiates a different radiation pattern. In other words, the radiation pattern of the DMA aperture undergoes spatio-temporal variation as the operating frequency is swept. In this paper, we use the term "mask" to refer each DMA aperture configuration represented by different radii of radiating elements. In this study we have considered twenty different masks and for each mask, the radii of elements are randomly considered between 0.9mm and 1.5mm. For analysis, the 20-22 GHz band is sampled at 101 discrete frequency points. The reflection coefficient (S_{11}) curves of the DMA are shown in Fig. 4. Here, the S_{11} curves of masks (1, 4, 8, 12, 16 and 20) are presented as an example. The radiation pattern of each mask is controlled by the collective contribution summed from each radiating CcELC element, as in [7].

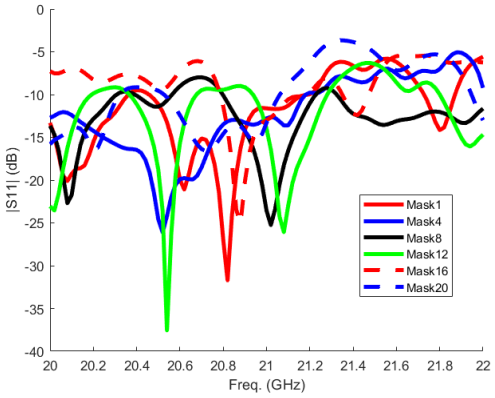

Fig. 4. DMA $|S11|$ parameters for masks: 1, 4, 8, 12, 16, 20.

2) *Receiver: Open-waveguide Probe (WR42)*

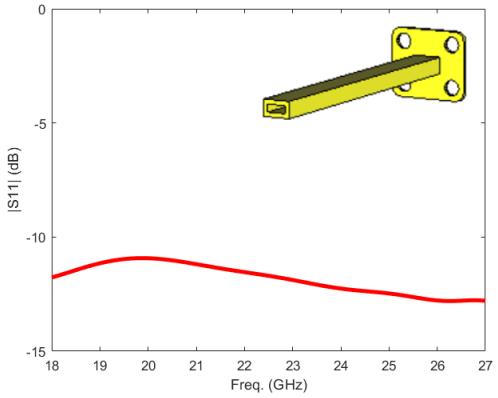

Fig. 5. WR42 waveguide probe: $|S_{11}|$.

Modelling of the receiver probe (WR42) is implemented in the full-wave EM CST Microwave Studio Platform. The S_{11} curve is presented in Fig. 5. The $|S_{11}|$ curve is less than -10dB over 18-27 GHz frequency band.

3) *Breast Cancer Modelling*

There are four stages (I through IV) of a tumour which can be described as different stages of the breast cancer [8]. The most common tool that doctors use to describe the stage is the TNM system which defines the dimension of a tumour [8]. Here, we are more interested in knowing the tentative size of tumours linked to different stages so that we can use this information in this study. Therefore, the associated size with different stages of tumours is listed in Table 1.

Table 1. Tumour Size.

T Stage	**Size**
T1	T1a: 1mm-5mm, T1b: 5mm-10mm, T1c: 10mm-20mm
T2	20mm-50mm
T3	$\geq 50mm$
T4	Spreading

Next, the breast structure can be modelled as three layers of tissues which mainly consists of the skin, fat, and tumour (or tumours) [4]. The model of an example breast structure with tumours is shown in Fig. 6 in the context of the imaging setup. The shape of the breast is modelled as a semi hemisphere and its considered diameter is 68 mm. The skin has a thickness of 4 mm, and the fatty region has a diameter equal to 60 mm. For simplicity, the whole shape is considered as a solid structure. Also, the dielectric properties reported by [3] of a normal breast tissue vary in an approximate 10% range around $\epsilon_r = 9$ and $\delta = 0.4S/m$ whereas for malignant tumours, $\epsilon_r = 50$ [4] and $\delta = 4S/m$. In CST Microwave Studio, the material library has also similar values for the breast tumour. Therefore, in this study we have considered the available information from the CST Microwave Studio for tumour modelling. The parameters used in this work are listed in Table 2.

Table 2. Electrical parameters of breast cancer

Tissue	**Permittivity F/m**	**Conductivity S/m**	**Density Kg/m^3**
Skin	36.7	2.34	1109
Fat	4.84	0.262	911
Tumour	54.9	4	1058

C. *Simulation Setup*

The configuration of the DMA and breast with a tumour is illustrated in Fig. 6. The distance between the breast and the antenna aperture is considered as 7λ. A significant advantage of the DMA aperture can be appreciated by investigating Fig. 6. As mentioned earlier, the size of the DMA aperture is 4λ. Conventional sampling of this aperture at the Nyquist limit would require 10 x 10 = 100 dedicated channels whereas the DMA aperture makes use of a single channel as depicted in Fig. 3. Each mask allows the measurements of the backscattered signals in spatially coded data to be post-processed for imaging.

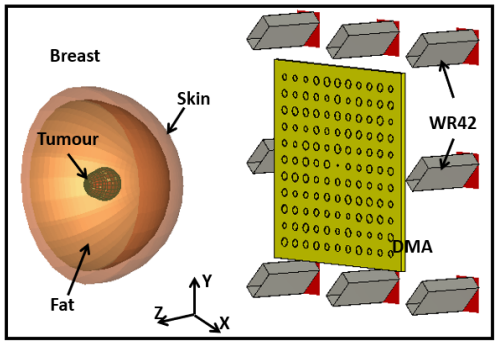

Fig. 6. Computational imaging system represents the breast tumour along with the DMA (Tx) and probes (Rx) designs.

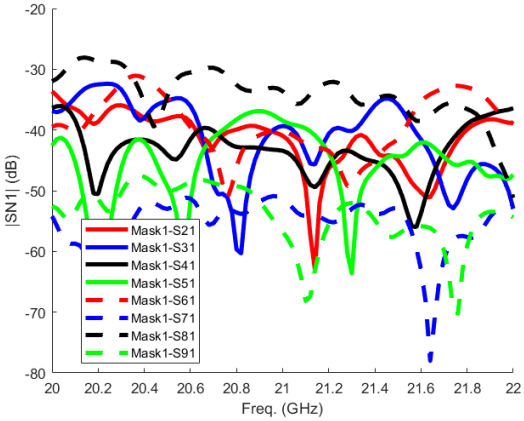

Fig. 7. Examples of backscattered signals collected between DMA and eight probes in Mask-1, and in $|SN1|$, N represents the Rx probes.

For each mask, all receiver probes collect the reflected signals as backscattered signals. This way, total 160 (20x8) backscattered signals (S_{21}) are used to decode the scene information. The backscattered signals due to the presence of tumours are shown in Fig. 7.

In this study, we used a spherical shaped tumour of radius 5 mm. The considered size belongs to the T1 stage as listed in Table. 1. Next, Eq. (2) is used to reconstruct the image using the matched-filtering technique.

III. Imaging Results

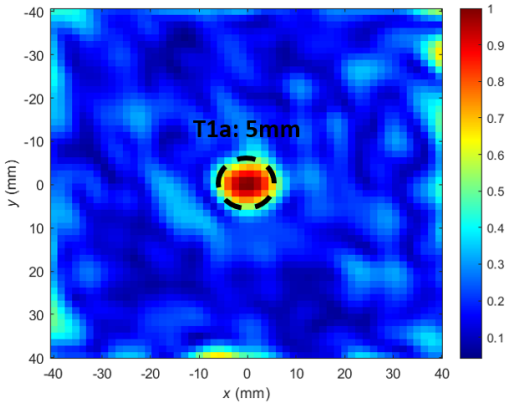

Fig. 8. Reconstructed image of breast cancer: T1-stage tumour located at (0mm, 0mm).

The reconstructed images are shown in Fig. 8. The reconstructed image indicates the presence of a T1 stage breast tumour. More specifically, the upper limit of T1b Stage is clearly detected in the reconstructed image.

The preliminary study shows an encouraging result for the detection of malignant tissues at a very early-stage of its growth. Further, it will be interesting the see the performance of the computational imaging in case of multiple discrete tumours.

IV. Conclusion

In this paper, we presented the preliminary study for detecting the breast cancer as an application of a computational imaging system operating at microwave frequencies. Based on the presented study, the computational imaging technique can detect the malignant tissues in the early stage of their growth using a DMA frontend architecture. The use of the DMA significantly simplifies the physical layer architecture and can help in reducing the overall system cost. Moreover, the early detection can significantly help the doctors to decide the best treatment for a patient, further increasing the chance of recovery.

Acknowledgment

This work was funded by the Leverhulme Trust under Research Leadership Award RL-2019-019.

References

[1] C. R. UK. Visited on 2022-03-21. [Online]. Available: https://www.cancerresearchuk.org/health-professional/cancer-statistics/statistics-by-cancer-type/breast-cancer#heading-Zero

[2] M. Mehranpour, S. Jarchi, A. Keshtkar, A. Ghorbani, A. Araghi, O. Yurduseven, and M. Khalily, "Robust breast cancer imaging based on a hybrid artifact suppression method for early-stage tumor detection," *IEEE Access*, vol. 8, pp. 206 790–206 805, 2020.

[3] S. Gabriel, R. W. Lau, and C. Gabriel, "The dielectric properties of biological tissues: II. measurements in the frequency range 10 hz to 20 ghz," vol. 41, no. 11, pp. 2251–2269, nov 1996. [Online]. Available: https://doi.org/10.1088/0031-9155/41/11/002

[4] Z. Wang, E. G. Lim, Y. Tang, and M. Leach, "Medical applications of microwave imaging," vol. 2014, no. 11, 2014.

[5] M. Elsdon, O. Yurduseven, and D. Smith, "Early stage breast cancer detection using indirect microwave holography," *Progress In Electromagnetics Research*, vol. 143, pp. 405–419, 2013.

[6] G. Lipworth, A. Rose, O. Yurduseven, V. R. Gowda, M. F. Imani, H. Odabasi, P. Trofatter, J. Gollub, and D. R. Smith, "Comprehensive simulation platform for a metamaterial imaging system," *Appl. Opt.*, vol. 54, no. 31, pp. 9343–9353, Nov 2015. [Online]. Available: http://opg.optica.org/ao/abstract.cfm?URI=ao-54-31-9343

[7] T. V. Hoang, V. Fusco, T. Fromenteze, and O. Yurduseven, "Computational polarimetric imaging using two-dimensional dynamic metasurface apertures," *IEEE Open Journal of Antennas and Propagation*, vol. 2, pp. 488–497, 2021.

[8] CancerNet. Visited on 2022-03-18. [Online]. Available: cancer.net/cancer-types/breast-cancer/stages